DMU

Advanced Journal of Interdisciplinary Studies 9(2025) 1595-1617

Journal homepage: www.ajids.dmu.edu.et

AJIDS

Volume 9(1), June 2025

Geospatial Analysis of Wetland Degradation and Its Consequences in the Muga Watershed, Upper Abay Basin, NorthEastern Ethiopia

Kiros Getachew Belachew[1,*], Abebaw Andarge Gedefaw[2], Berhanu Tadesse Beyene[1]

[1]Department of Natural Resource Management, College of Agriculture and Natural Resources, Debre Markos University, POBox 269, Debre Markos, Ethiopia
[2]Institute of Land Administration, Debre Markos University, Debre Markos, Ethiopia

[*]Corresponding author email: Kiros_getachew@dmu.edu.et

Abstract

This study examines wetland degradation in the Muga Watershed, Upper Abay Basin, Ethiopia, over a 35-year period (1986–2021). It addresses critical gaps in understanding wetland loss, its drivers and consequences by leveraging geospatial analysis and remote sensing techniques. Using Landsat satellite imagery, Land Use/Land Cover (LULC) changes were detected through a GIS-based approach with the Maximum Likelihood Classification (MLC) method. The classification achieved an overall accuracy of 88.5% and a kappa coefficient of 0.85, ensuring reliable results. Statistical analyses further validated classification accuracy. Field surveys and key informant interviews identified the primary drivers of wetland loss and its impacts. Results showed notable land cover changes: wetlands, forests, and grasslands declined by 12.42%, 9.62%, and 5.58%, respectively, while agricultural land and built-up areas expanded by 26.54% and 1.09%. The major drivers of wetland degradation included population growth (98.1%), agricultural expansion (92.5%), and overgrazing (93.8%). Key consequences included increased flooding and erosion, biodiversity loss, reduced crop yields, declining water quantity and quality, resource conflicts, and climate change impacts. This study underscores the urgent need for integrated land-use planning, community education, and stronger policy interventions to mitigate wetland degradation and ensure long-term environmental sustainability. By applying advanced geospatial techniques, this research provides critical insights into wetland loss, contributing to more effective conservation and management strategies.

Keywords: Geospatial Analysis; Land use/land cover change; Maximum Likelihood; Supervised Image Classification; Wetland Degradation

1. Introduction

Wetlands, situated at the dynamic interface of land and water, are vital ecosystems that provide a diverse array of essential services. These include water purification, flood regulation, carbon sequestration, and critical habitats for biodiversity. Beyond their ecological importance, wetlands are integral to sustaining local livelihoods, particularly in agrarian societies, by supporting agriculture, grazing, and water supply. Despite their immense value, wetlands have been experiencing widespread degradation on a global scale, with the rate of loss accelerating in recent decades. This degradation is predominantly driven by agricultural expansion, urbanization, population growth, and climate change (Ballut-Dajud et al., 2022). Sub-Saharan Africa, including Ethiopia, has been significantly affected by these pressures, resulting in the substantial loss of wetlands and the ecosystem services they provide (Dube et al., 2023).

In Ethiopia, wetlands cover approximately 2% of the national land area and are critical for maintaining environmental sustainability and supporting local livelihoods. However, unsustainable land-use practices, weak governance, and limited public awareness have contributed to their rapid decline (Dixon et al., 2021). Research from different regions of Ethiopia underscores the severity of wetland degradation. For example, In the Central Rift Valley, Murtessa (2020) identifies pollution and unsustainable water withdrawals as major threats, while Temesgen et al. (2025) report sedimentation and invasive species as key drivers of wetland degradation in the Genale Dawa River Basin, in the southern part of Ethiopia. In the Amhara region, in the Lake Tana Basin, population growth and land scarcity have driven widespread conversion of wetlands into agricultural land (Minale & Belete, 2017). Similarly, studies in the Fogera Plain by Zenebe et al. (2022) highlight declining water tables and intensive farming as exacerbating factors. Collectively, these studies demonstrate that wetlands across Ethiopia face diverse anthropogenic and environmental pressures, with profound ecological and socio-economic consequences.

The Muga Watershed, located in the Upper Abay Basin of the Amhara region, exemplifies these challenges. Wetlands in this watershed play a pivotal role in supporting agriculture, grazing, and water supply, forming the backbone of local livelihoods. However, rapid agricultural expansion, unmanaged grazing, and population growth have placed immense pressure on these ecosystems (Belay & Mengistu, 2019). Despite the critical importance of these wetlands, there is a notable lack of research on their spatial and temporal dynamics, the drivers of their degradation, and the resulting consequences. While studies in Amhara and other regions of Ethiopia have provided valuable insights into wetland loss, the absence of long-term geospatial analysis specific to the Muga Watershed creates a critical knowledge gap, hindering effective conservation and management efforts.

This study aims to fill this gap by analyzing the spatial and temporal dynamics of wetlands in the Muga Watershed over a 35-year period using Geographic Information Systems (GIS) and Remote Sensing (RS) technologies. Furthermore, it seeks to identify the key drivers of wetland degradation and evaluate the ecological and socio-economic consequences of these changes. By addressing these objectives, the study provides essential insights to inform policy and conservation strategies, contributing to the sustainable management of wetlands in the Muga Watershed and beyond.

2. Materials and Methods

2.1.Description of the Study area

The Muga watershed is located in the Upper Blue Nile Basin, which is approximately 248 km northwest of Addis

Ababa, between the towns of Dejen and Bichena. This watershed is one of the choke mountain watersheds in the Northern Highlands of Ethiopia. Geographically, it is situated between 10°6’30″’’ to 10°43’30’’ North latitude and 37°49’00’’ to 38°16’30’’″ East longitude (Figure 1). It covered an area of 696.61 km². The study area is mainly found in Debay Tilat Gin district, East Gojjam Zone and Amhara Regional National State some of area found in Enemay and Dejen district. It is bordered with Bibugn and, Sinan in West, Dejen and Enemay district in East, Awabl in South and Sedi in North. Muga River is the main perennial river that originates in the Bibugn district near Choke Mountain at an elevation of 4084 m.a.s.l. and drains into the upper Blue Nile River. When it reaches the Blue Nile River, Muga's agroclimatic zone is classified as wet/moist dega (temperate-like climate-highlands with 2500-3000 meters altitude) and kola (hot and desert type, less than 1500 m in altitude).

There is high spatial and temporal variation in rainfall in the study area. There is one long rainy season, from June to September, with the maximum precipitation occurring in August. The main rainfall season, which accounts for approximately 70-90% of the annual rainfall, occurs from June to September, while small rains also occur from December to March. The average temperature in the area ranges from 5°C to 33.5°C.These environmental factors, coupled with the region’s socio-economic dynamics, are crucial in understanding land-use changes and wetland dynamics.

According to the Debaytilatgin Woreda Agriculture Office (2016), the local population relies predominantly on agriculture, including rain-fed and irrigated farming, livestock grazing, and, to a lesser extent, forest products. Rapid population growth, land tenure changes (such as rural land certification), and urbanization have placed increasing pressure on wetlands and other natural resources, driving land use changes over the past decades.

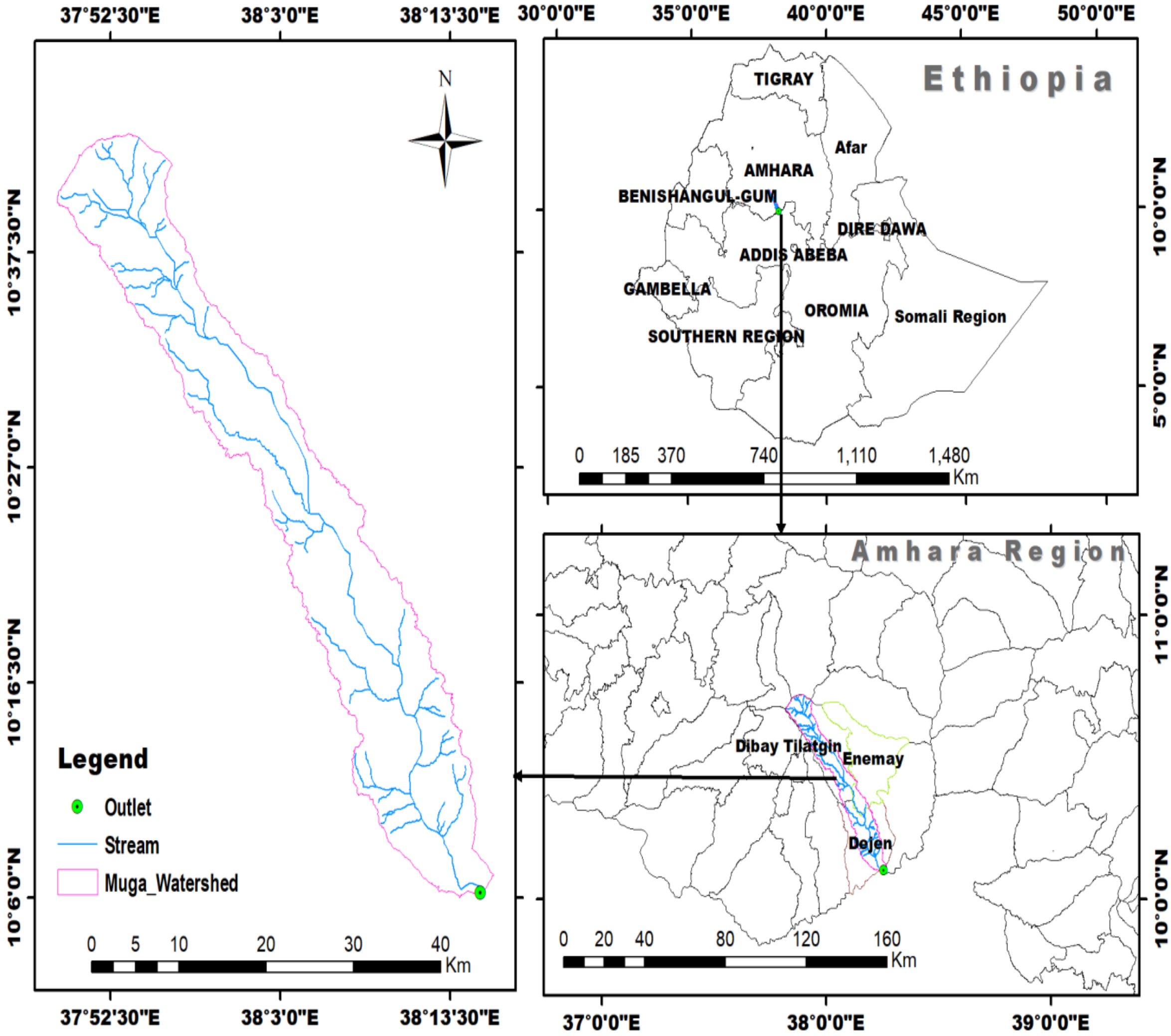

Figure 1. Muga Watershed Study area

2.2.Methods

2.2.1. Remote Sensing Data and Pre-processing

This study employed time-series spatial data to examine land use/land cover. Satellite images from the Landsat 4-5 Thematic Mapper™ from 1986, 1998, and 2010 and Landsat 8 Operational Land Images (OLI) from 2021 were used to produce land use/land cover maps. The selection of years was aligned with the key historical events. That is, the year 1986 was selected as the reference year pre-1991 government change, and 1998 was assumed as pre-rural land certification that was launched in 2002. 2010 was selected as post-land certification and 2021 was selected to obtain the current status of the land use/land cover of the study area. Multi-temporal Landsat satellite images of the study area were freely downloaded from the United States Geological Survey (USGS) Earth Explorer portal for all four time periods (https://earthexplorer.usgs.gov/) (accessed on January 10, 2024). Datasets taken in the dry season (January to February) were selected for the dry season (January-February) to reduce seasonal variation Kindu et al. (2013), ensuring optimal vegetation clarity, spectral distinction, and cloud-free satellite imagery as well as to record land surface reflectance values that were not influenced by agricultural practice for training and classification.

Image preprocessing techniques were applied to correct image distortions, remove noise, and improve image data interpretability. In particular, appropriate band selections, atmospheric and geometric corrections, subsetting productions, layer stacking, and image enhancements have been applied (Chamling & Bera, 2020). L5 TM images were registered to their corresponding Landsat 8 OLI images using automated image-to-image registration approaches and a set of ground truth points (GTPs) to combine time-series image datasets to enable change detection at the pixel level. The Aster Global DEM (30m) was used for landscape mapping, supplemented by additional ancillary data. The specifications of the datasets used in the investigation are listed in Table 1.

Table 1. Satellite Image Overview

Satellite images	Date of acquisition	Path	Row	Resolution	Sources
Landsat 4-5	28/01/1986	169	53	30m	USGS Website
	29/01/1998	169	53	30m	USGS Website
	30/01/2010	169	53	30m	USGS Website
Landsat 8 /OLI/	13/02/2021	169	53	30m	USGS Website
DEM				30m	Aster global DEM Website

2.2.2. Field Data Collection

Ground-reference data were gathered for the training and validation of land-cover types in the study area. Following Chanda and Majumder (2011), a minimum of 50 samples per class were targeted, with at least 80 samples for each of the five defined classes (Table 2): forest, grassland, agricultural land, built-up areas, and wetlands (Girma et al., 2022).

Table 2. Land Use/Land Cover Class Description

LULC classes	Description
Wetlands	Areas where the water level is permanently or temporarily at (or very near) the land surface typically covered in either herbaceous or woody vegetation cover.
Settlement/built up	Areas where there is a permanent concentration of people, buildings, and other man-made structures and other activities.
Forest area	Areas covered by trees forming closed or nearly closed canopies (70-

	100%)
Grassland	Areas with permanent grass cover along ridges steep slopes and plain areas, used for grazing; usually private as well as communal.
Agricultural land	Contiguous areas used for rain-fed and irrigated cultivation, including fallow plots, cultivated land mixed with some bushes, trees and rural homesteads but dominated by farmland.

Source: Adopted from (Di Gregorio & O'BRIEN, 2012)

Representative training sites for image classification and validation (accuracy assessment) were collected for each land use/land cover class. Land-use/land-cover classification was performed for each acquisition date. Reference data for 1986, 1998, and 2010 were collected through visual interpretation from Google Earth Time-lapse, using pure pixels of 30 m × 30 m for each land cover type. A total of 2,054 reference data points were collected for these years, with 800 used for classification and 1,254 for accuracy assessment. Reference data for 2021 were gathered via field surveys using a handheld GNSS device (Garmin GPS MAP 60 CSx). The sample locations were selected based on accessibility or convenience. To ensure representative sampling, 3,000 samples were collected using the random sampling technique for the land use/land cover classification of 2021, with 1,000 used for training and 2,000 for accuracy evaluation. As reference data, historical black and white aerial photos were combined with raw satellite imaging data via visual interpretation to collect sample points for classifying the Landsat images from 1986, 1998, and 2010. Along with the training data collection, transect walks were used to conduct site observations, which were used to refine the training sites and verify the classified images. Considering the time lag between the acquisition date of satellite images and the assessment of reference data (Google Earth data and field survey), the reliability of reference data was verified in group discussions and interviews with elderly farmers because know the area better. In addition, Focus Group Discussions (FGDs) and Key Informant Interviews (KIIs) were conducted to complement quantitative changes in land use/land cover analysis.

2.2.3. Data Processing and Analysis

Land cover classifications for the four time periods (1986, 1998, 2010, and 2021) were conducted using supervised pixel-based classification with a GIS-based Maximum Likelihood Classifier (MLC) (Lillesand et al., 2015). This technique was chosen because it assumes a normal distribution of point clouds and computes the statistical probability of a given pixel value belonging to a particular land-cover class. In addition to reflectance values, the tool considers the covariance of the information contained in the sensors' spectral bands for land cover classes (Gupta, 2017). This approach also has a higher probability of weighting minority classes, which can be overshadowed by larger classes during sample training from the images.

Supervised classification relies on reference data where the land cover is known. Spectral signatures were derived from the reference data for each of the seven land cover types. Based on this data, a Maximum Likelihood Classification was applied to produce land cover maps for 1986, 1998, 2010, and 2021 for the entire study area.

Post-classification enhancement was performed to increase classification accuracy and reduce misclassifications (Harris & Ventura, 1995). During the post-classification, smoothing algorithms were applied using a majority filter. This involves passing a moving window through the classified dataset and determining the majority class within the window.

2.2.4. Accuracy Assessment for Image Classification

Accuracy assessment involves comparing classified data to trusted geographical data to evaluate classification performance. A confusion matrix was used for this purpose, with rows representing the classified values and columns representing field observations. The diagonal elements indicate the correctly classified pixels. The overall accuracy is calculated by dividing correctly classified pixels by the total, while the producer and user accuracy indices assess class-specific performance.

The Kappa coefficient, ranging from 0 to 1, measures agreement, with values above 0.8 indicating strong agreement, 0.4 to 0.8 moderate agreements; and below 0.4 poor agreement (Harris & Ventura, 1995). The reasons for these errors may include the similarity of the reflectance of settlement, grazing land, and cultivated areas. In addition, the rapid land use and land cover dynamic nature of the area may also introduce classification errors.

$$\acute{K} = \frac{\text{Observed accuaracy} - \text{chance agreement}}{1 - \text{chance agreement}} \ldots\text{(Eq.1)}$$

In reality, the value of $\check{K}$ usually ranges between 0 and 1. Kappa coefficient is calculated as follows:

$$\acute{K} = \frac{N\sum_1^k xii - \sum_1^k (xi+xx+i)}{N^2 - \sum_1^k (xi+xx+i)} \ldots\ldots\ldots\ldots\text{(Eq.2)}$$

Where: N is the total number of observations in the entire error matrix, k is the total number of classes or categories; xii refers to the number of observations correctly classified for a particular category, and $xi+$ and $x+i$ refer to the marginal totals for row i and column i associated with the category.

2.2.5. Wetland Change Analysis

Wetland changes were analyzed across four periods, 1986–1998, 1998–2010, 2010–2021, and 1986–2021, using cross-tabulation, following the approach of Zewdie and Csaplovies (2015). Percentage changes for each land cover type were calculated using the method described by Gashaw et al. (2018), assessing specific class gains, losses, and net changes, consistent with the approach of Alo and Pontius Jr (2008). The annual change rates for each land cover type were computed using the formula outlined by Puyravaud (2003).

Post-classification comparison provided a change matrix (Xu et al., 2018), with statistics presented in hectares and percentages. The rate of change (R) was determined using the formula:

Rate of change (R)= $\frac{X-Y}{T}$

Where R= Rate of change,

Y=initial year land use/ land cover in ha,

X= recent year land use/ land cover in ha,

T= time interval between initial and recent years (Geist et al., 2006)

The formula was used to calculate the rate of land use/land cover change in different studies (Degife et al., 2019; Hussien et al., 2018; Nishri, 2011; Teshome & Kinahan, 2011)

2.2.6. Socio-Economic Data Collection and Analysis Methods

2.2.6.1. Driving Force and Consequences of Wetland depletion

Primary data were collected via household surveys, key informant interviews, and direct observations to assess the driving forces and consequences of wetland degradation. A two-stage sampling method targeted the villages of Kuy Zuria, Asinadabo, Wodeb Eyesus, and Debre Eyesus, with 160 households randomly selected from 274 total numbers of households to ensure proportional representation across kebele (Cochran, 1977). Data were collected from April 25 to September 20, 2022, using a semi-structured questionnaire addressing the demographics and perceptions of wetland dynamics. The analysis included descriptive statistics with SPSS version 20 and qualitative insights from eight purposefully selected informants analyzed thematically.

3. Results and Discussion

3.1. Results

3.1.1. Accuracy Assessment of Land Cover Maps

The accuracy of the classified images was assessed using a confusion matrix with randomly selected reference points. Table 3 shows the overall accuracies for 1986, 1998, 2010, and 2021 at 86.1%, 87.6%, 89.9%, and 92.4%, respectively. Producer's accuracy ranged from 60% to 98.75%, the lowest in built-up areas due to spectral similarity, whereas the user's accuracy ranged from 78.24% to 100%, with the lowest for agricultural land due to its highly variable and dynamic nature. All maps had kappa coefficients above 0.80, indicating very good agreement with the ground truth. This accuracy met the requirements for further analysis and change detection, successfully identifying trends, and supporting qualitative comparisons.

Table 3. Accuracy Assessment of Land Cover Maps (1986-2921)

	Year							
	1986		1998		2010		2021	
Land cover type	User's (%)	Producer's (%)	User's (%)	Producer's (%)	User's (%)	Producer's (%)	User's (%)	Producer's (%)
Wetland	100.00	82.84	95.70	82.41	88.79	87.96	90.85	85.8
Agricultural	78.24	90.48	85.71	93.13	90.21	95.37	94.67	98.75

land								
Forest	91.48	78.92	92.62	74.83	91.09	90.64	91.72	83.72
Grassland	84.94	89.52	85.55	90.24	90.00	83.94	80.00	82.19
Built-up	100.00	66.67	100.00	60.00	81.25	61.90	90.91	85.71
Overall Accuracy	86.1%		87.6%		89.9%		92.4%	
Kappa coefficient	0.81		0.82		0.86		0.88	

3.1.2. Land Use / Land Cover in Muga Watershed

Figure 2 and Table 4 depict the results of the Land Use/land cover maps in the Muga watershed for the four reference years (1986, 1998, 2010, and 2021). Table 4 shows quantitative information about land use/land cover in the respective years.

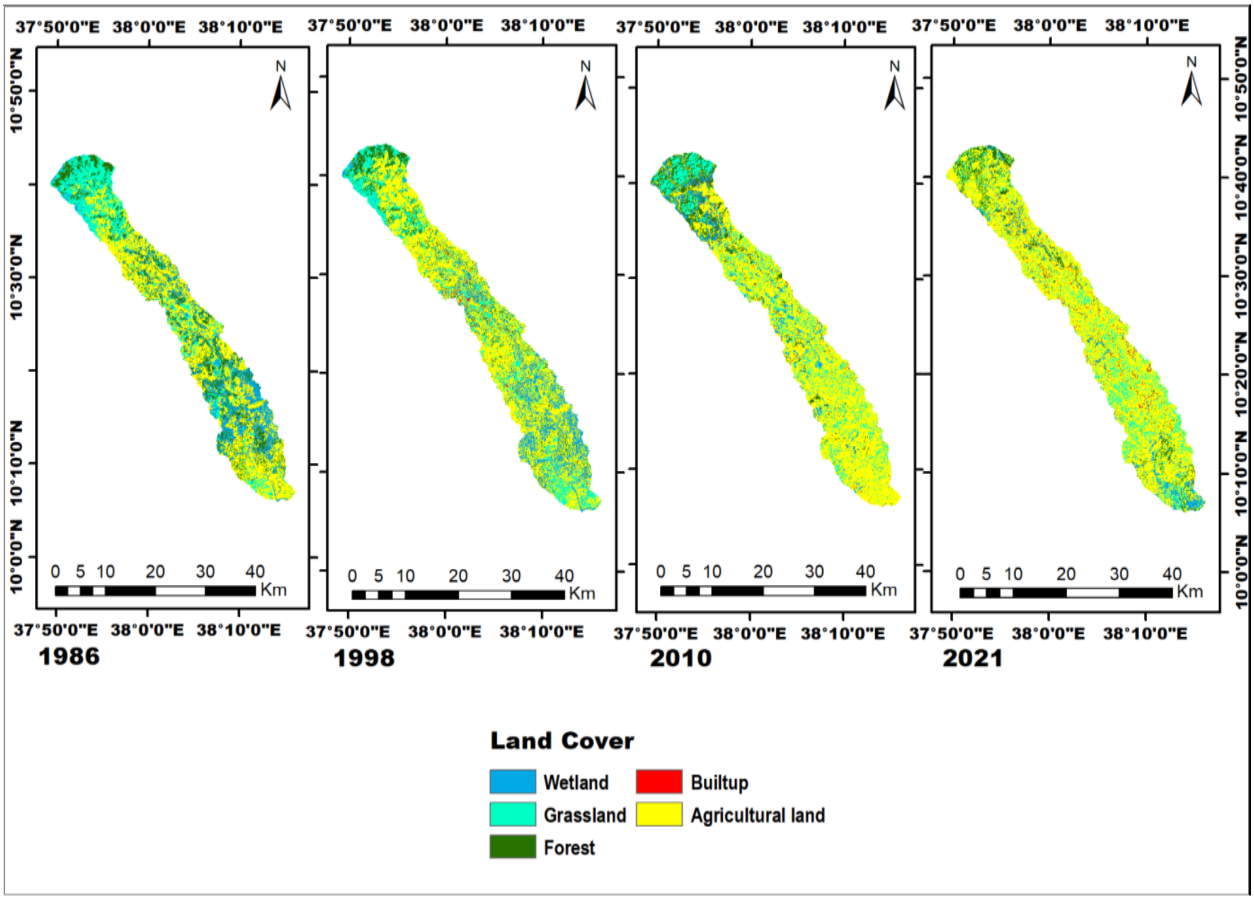

Figure 2. Land Use/Land Cover Maps of Muga Watershed for 1986, 1998, 2010, and 2021

Table 4. Area Coverage of Classified Land Cover Categories (1986, 1998, 2010, and 2021)

Land cover type	Area							
	1986		1998		2010		2021	
	(ha)	(%)	(ha)	(%)	(ha)	(%)	(ha)	(%)
Wetland	13226.49	18.71	11709.81	16.57	6262.83	8.86	4447.62	6.29
Agricultural land	30452.4	43.08	38516.94	54.49	45434.88	64.28	49209.4	69.62
Forest	11858.67	16.78	6521.76	9.23	6234.03	8.82	5059.08	7.16
Grassland	14697.45	20.79	13307.94	18.83	11935.26	16.89	10750.9	15.21
Built-up	447.75	0.63	626.31	0.89	815.76	1.15	1215.81	1.72
Total	70682.76	100	70682.76	100	70682.76	100	70682.76	100

As illustrated in Table 4, agricultural land was the predominant land-cover type in the study watershed. The 1986 Land Use/Land Cover map revealed that agricultural land occupied 43.08% of the watershed area, followed by grassland (20.79%), and wetland (18.71%). Forest and built-up areas comprised 16.78% and 0.63% of the watershed, respectively. By 2021, the Land Use/Land Cover map indicated that agricultural land had increased to cover 69.62% of the watershed. Grassland decreased to 15.21%, and wetland reduced to 6.29% and forest declined by 7.16%. Meanwhile, the built-up areas expanded to 1.72%.

3.1.3. Land Cover Changes

Table 4 details the land cover changes in the Muga Watershed from 1986 to 2021, highlighting shifts across four periods: 1986-1998, 1998-2010, and 2010-2021. A significant reduction of 8,778.87 ha changes impacted wetland ecosystems from 1986 to 2021. So, the land use/land cover change in the periods 1986 to 2021 showed that, agricultural land increased from 30,452.4 ha to 49,209.4 ha, and built-up areas rose from 447.75 ha to 1,215.81 ha. Conversely, wetlands, grasslands, and forests decreased from 13,226.49 ha, 14,697.45 ha, and 11,858.67 ha to 4,447.62 ha, and 10,750.9 ha to 5,059.08 ha, respectively (Table 4).

Over the past 35 years, agricultural land and built-up areas have grown at annual rates of 0.76% and 0.03%, respectively, while wetlands, grasslands, and forests have declined at rates of 0.35%, 0.16%, and 0.27%, respectively. From 1986-1998, agricultural land increased by 11.41% (620.35 ha/year), 9.79% (576.5 ha/year) from 1998-2010, and 5.34% (314.54 ha/year) from 2010-2021. Built-up areas grew by 0.25%, 0.27%, and 0.57% during the same period. From 1986-1998, Wetlands decreased at rates of 2.5% (116.67 ha/year), 7.71% (453.92 ha/year), from 1998-2010, and 2.57% (151.27 ha/year) from 2010-2021. Forests declined by 7.55%, 0.41%, and 0.57%, whereas grasslands decreased by 1.97%, 1.94%, and 1.68%, respectively, in the same period (Table 5).

Overall, from 1986 to 2021, agricultural land and built-up areas increased by 521.03 ha/year and 21.34 ha/year, while wetlands, forests, and grasslands decreased by 243.86 ha/year, 188.88 ha/year, and 109.63 ha/year, respectively (Table 5).

Table 5. Change Metrics for Classified Land Cover (1986-2021)

Land Cover type	Change (%)				Net change (ha)				Rate of change (ha/year)			
	1986-1998	1998-2010	2010-2021	1986-2021	1986-1998	1998-2010	2010-2021	1986-2021	1986-1998	1998-2010	2010-2021	1986-2021
Wetland	-2.15	-7.71	-2.57	-12.42	-1516.68	-5446.98	-1815.21	-8778.87	-116.67	-453.92	-151.27	-243.86
Agricultural land	11.41	9.79	5.34	26.54	8064.54	6917.94	3774.52	1875.7	620.35	576.50	314.54	521.03
Forest	-7.55	-0.41	-1.66	-9.62	-5336.91	-287.73	-1174.95	-6799.59	-410.53	-23.98	-97.91	-188.88
Grassland	-1.97	-1.94	-1.68	-5.58	-1389.51	-1372.68	-1184.36	-3946.55	-106.89	-114.39	-98.70	-109.63
Built-up	0.25	0.27	0.57	1.09	178.56	189.45	400.05	768.06	13.74	15.79	33.34	21.34

3.1.4. Wetland Change Analysis

Wetlands decreased from 13,226.49 ha in 1986 to 4,447.62 ha in 2021, with an overall loss rate of 243.86 ha/year (Figure 3). The most significant decline occurred between 2010 and 2021, with a loss of 1,815.21 ha due to land certification and farmland expansion. Annual loss rates varied: 126.39 ha/year (1986-1998), 453.92 ha/year (1998-2010), and 165.02 ha/year (2010-2021). Overall, wetlands, grasslands, and forests significantly diminished during this period.

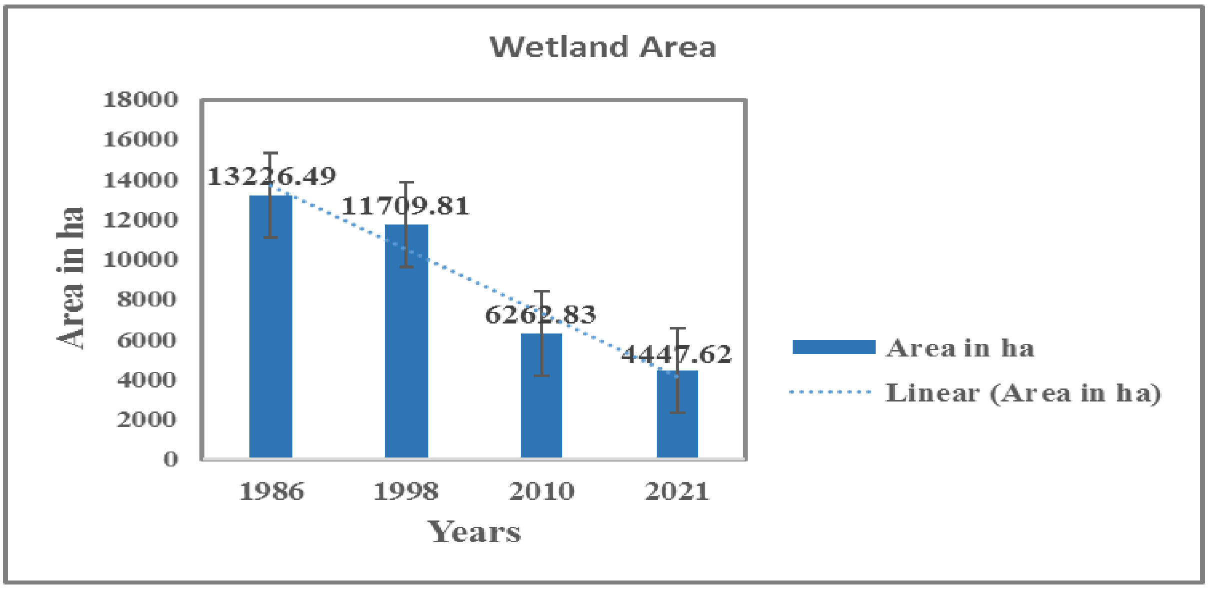

Figure 3. Total Wetland Change Over time (in ha)

3.1.5. Land use/land Covers Change Detection

Table 6 and Figure 4 present transitions in Land Use/Land Cover from 1986 to 2021, with diagonals showing persistence and off-diagonals indicating conversion. Significant shifts from 1986 to 2021 were identified, highlighting the need to understand the classes that are transitioning, which is essential for management decisions. A pixel-by-pixel comparison of images reveals both the direction of change and stable land cover types.

For the Muga watershed, wetlands have been notably converted to farmland over the past 35 years. Approximately 9,013.68 ha of wetlands have transitioned to farmland, with 131.85 ha to built-up areas (Table 6). This indicates that farmland expansion and overgrazing negatively affected wetlands.

From 1986 to 2021, 68.15% of wetlands have shifted to agricultural land, 21.36% to grassland, 5.98% to forest, and 1% to built-up areas (Figure 4). Population pressure (98.1) is a key driver of agricultural expansion, contributing to wetland loss (Table 7).

Table 6. Conversion Matrix of Land Use/Land Cover Changes (1986-2021)

		Land cover 2021					
		AL	B	F	GL	WL	GT
Land cover 1986	AL	22803.84	683.1	1090.35	3763.08	2112.03	30452.4
	B	208.45	138.32	16.02	59.76	25.2	447.75
	F	7260.66	124.83	1551.69	2086.29	835.2	11858.67
	GL	9797.76	262.71	1609.83	2016.45	1010.7	14697.45

WL	9013.68	131.85	791.19	2825.28	464.49	13226.49
GT	49084.39	1340.81	5059.08	10750.86	4447.62	70682.76

Key: AL= Agricultural land, B= Built-up, F= Forest GL=Grassland, WL=Wetland, GT= Grand Total

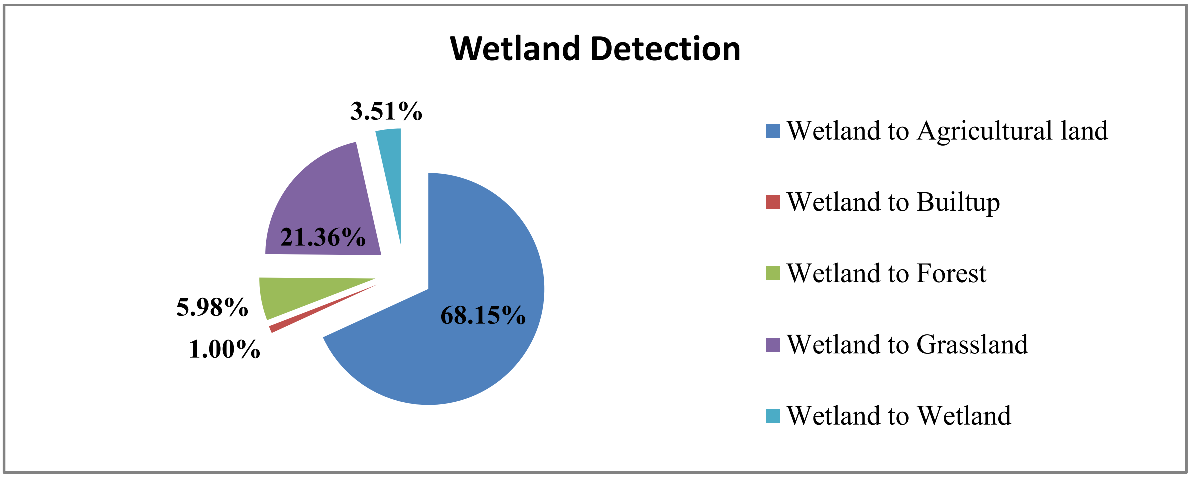

Figure 4. Wetland detection from 1986-2021

3.1.6. Drivers of wetland change

Household farmers reported that wetland depletion was influenced by various factors, and the results are presented in Table 7.

3.1.6.1.Household Characteristics

Interviews with 160 respondents revealed that 76.3% were male and 23.7% female. Age distribution was: 8.1% (20-30), 18.1% (31-40), 42.5% (41-50), and 31.3% (51+). Occupations included farmers (50.8%), trade and retail (18.8%), construction workers (17.7%), and craft (12.7%).

3.1.6.2.Driving force of wetland change

According to the data collected from the household survey, significant factors affected wetland depletion. That is, the majority of respondents (98.1 %, 93.8 %, and 92.5 %) perceived that population growth, overgrazing, and farmland expansion, respectively, affected wetland depletion (Table 7). Population growth drives other issues, leading to practices such as water diversion and waste dumping, which further diminish wetland areas.

Table 7. Perceived Driving Force of Wetland Changes by Household Farmers

Variables	**Yes**		**No**	
Drivers of Wetland change	Number of respondent	%	Number of respondent	%
Population Growth	157	98.1	3	1.9
Farmland expansion	148	92.5	12	7.5
Sedimentation	108	67.5	52	32.5
Overgrazing	150	93.8	10	6.2

Lack of Rainfall	125	78.1	35	21.9
Eucalyptus tree plantation	118	73.8	42	26.2
Waste Disposal	126	78.7	34	21.3

* Total number of cases was 160 and due to a multiple response question, multiple counts are possible.

3.1.7. Consequences of Wetland degradation

The household survey, complemented by key informant interviews, revealed several significant and interconnected consequences of wetland degradation in the study area. The most critical impact was the increased occurrence of flooding and erosion, reported by 95 % of respondents, emphasizing the heightened vulnerability of the region to these hazards. This was closely followed by the loss of biodiversity, with 93.7 % of respondents observing a decline in wild flora and fauna (Table 8). The reduction in biodiversity disrupts essential ecosystem services and has cascading effects on the local environment and livelihoods.

Wetland degradation has also severely impacted agriculture, with 91.3 % of respondents reporting a decline in crop yields. This reduction not only threatens food security but also creates economic challenges for communities reliant on farming as their primary livelihood. Furthermore, water scarcity emerged as a pressing issue, as 90 % of respondents cited shortages in both the quantity and quality of water during the dry season. Additionally, 80 % of respondents noted the drying of water bodies, further compounding the region's water-related challenges.

Socio-economic impacts were also significant. Approximately 82.5 % of respondents reported conflicts over resource utilization, reflecting increased competition for dwindling resources. Furthermore, 88.7 % of respondents linked wetland degradation to the impacts of climate change, underlining the broader vulnerability of the area to environmental and climatic shifts.

Overall, these findings highlight the extensive consequences of wetland degradation, affecting both the natural environment and local communities. Flooding, erosion, biodiversity loss, water scarcity, and socio-economic tensions stand out as critical challenges. These results point to the urgent need for strategies aimed at conserving and restoring wetlands to preserve ecosystem services, mitigate climate risks, and support the livelihoods of affected populations.

Table 8. The consequence of wetland degradation in the study area

Consequences	Yes		NO	
	Number of respondents	%	Number of respondents	%
Occurrence of flood and erosion	152	95	8	5
Decrease of Crop yield	146	91.3	14	8.7

Loss of biodiversity (wild flora and fauna)	150	93.7	10	6.3
Shortages of quality and quantity water	144	90	16	10
Drying of water bodies	128	80	32	20
Conflict over resource utilization	132	82.5	28	17.5
Occurrence of Climate change	142	88.7	18	11.3

3.2. Discussions

3.2.1. Land Cover change

The Muga watershed has experienced significant land cover changes from 1986 to 2021, as detailed in the land cover maps for 1986, 1998, 2010, and 2021 (Table 4 and Figure 2). This study identified five primary land cover types: agricultural land, built-up areas, grasslands, forests, and wetlands. Wetland loss was most pronounced during the period from 2010 to 2021, with decreases of 1,516.68 ha, 5,446.98 ha, and 1,815.21 ha in the periods 1986–1998, 1998–2010, and 2010–2021, respectively.

Agricultural land has expanded significantly from 43.08% in 1986 to 69.62% in 2021 (Table 4). This pattern reflects the similar trends observed in the upper Blue Nile Basin (Belay & Mengistu, 2019), especially following the land certification reforms of the 1990s. Such agricultural expansion is also evident across Ethiopia's highlands (Gessesse et al., 2019; Hassen & Assen, 2018), often at the expense of the environment. The demand for increased food production, compounded by limited access to alternative livelihoods, has led to extensive conversion of wetlands into farmland.

Built-up areas increased from 447.75 ha in 1986 to 1,215.81 ha in 2021 (Table 4), encroaching on agricultural land, grasslands, and wetlands. This growth reflects the rising demand for rural settlements and public infrastructure, a trend consistent with the urbanization patterns observed in the upper Blue Nile Basin (Belay & Mengistu, 2019) and Gozamin district (Gedefaw et al., 2020). As in many parts of the world, urban expansion has exacerbated wetland loss, as areas covered by wetlands are transformed into infrastructure zones, such as roads, buildings, and other urban developments.

Similar patterns of wetland degradation have been reported globally, with wetlands often being drained or converted for agricultural and urban purposes (Barbier, 2011; Kingsford et al., 2016). The loss of approximately 12.42% of wetlands in the Muga watershed is due to agricultural expansion, overgrazing, and urban growth (Table 5), which is consistent with findings from Lake Abaya-Chamo (Zekarias et al., 2021) and other Ethiopian wetlands. The Gumara Watershed also experienced significant wetland loss from 1957 to 2005 (Wubie et al., 2016). This is also aligned with global trends, where wetlands are rapidly shrinking owing to human activities, leading to biodiversity loss, soil erosion, and disruptions in the water cycle.

Forest cover in the Muga watershed has decreased from 16.78% in 1986 to 7.16% in 2021 (Table 4 and Figure 5), primarily because of deforestation driven by agriculture, urban expansion, and fuelwood collection. This decline mirrors broader trends across Ethiopia and the Horn of Africa, where forests continue to shrink for similar reasons (Kindu et al., 2013; Zeleke & Hurni, 2001). On a global scale, forest loss remains a critical issue, as forests are vital for regulating climate and maintaining biodiversity (Kumar et al., 2022).

Grasslands also experienced a decline of 3,946.55 ha between 1986 and 2021 (Table 5), primarily due to conversion for farming and urbanization—trends observed globally in many regions (Biró et al., 2013) and other studies in Ethiopia (Gedefaw et al., 2020; Wubie et al., 2016).

3.2.2. Driving force of wetland change

Wetland changes in the Muga Watershed are influenced by multiple factors identified by the household survey and key informants, including population growth, agricultural expansion, overgrazing, waste disposal, reduced rainfall, eucalyptus plantations, and sedimentation (Table 7, Figure 5 and 6). Over 98% of the respondents cited population growth as a key driver, consistent with previous studies linking population increases to wetland encroachment in Ethiopia (Simane et al., 2013).

.

A previous study showed a 90% increase in the settlement area around Lake Abaya-Chamo from 1990 to 2019, reducing wetland cover (Zekarias et al., 2021). Ethiopia's population growth rate of 2.4% exacerbates land cover changes, with agricultural development and livestock grazing being significant socioeconomic drivers (Mathewos et al., 2022). Studies in the Northern Central Highlands indicate that agricultural expansion is converting wetlands to farmland, contributing to the decline of swamp areas (Hailu et al., 2020)

Additionally, overgrazing compacts soils and diminishes the water retention capabilities of wetlands (Zekarias et al., 2021). Other factors influencing land-use dynamics include sedimentation, eutrophication, pollution, resource overuse, and poor catchment management(Giweta & Worku, 2018; Simane et al., 2013; Tegaye, 2009) Urban expansion has also contributed to wetland loss, with a reported 6.4% reduction in lake area and a 42.7% decrease in wetland coverage over 45 years (Assefa et al., 2021). Overall, land-use changes are closely linked to socioeconomic dynamics, as population growth drives the demand for cultivated land, grazing areas, and settlement space (Melese, 2016).

Figure 5. Eucalyptus tree landscape with nearby settlement adjacent to the wetland

Source: Own source

Figure 6. Agricultural land encircling the wetlands

Source: Own source

3.2.3. Consequences of Wetland Degradation in the Muga Watershed

The findings from the Muga Watershed closely align with research conducted in several wetland areas across Ethiopia, particularly in the Amhara region, as well as in other parts of the country. A key environmental consequence of wetland degradation in the Muga Watershed is the increased flooding and erosion, with 95% of respondents reporting these issues. This reflects the findings of Agidie et al. (2024), who studied the Lake Tana Basin in the Amhara region. Their research found that wetland loss in the Lake Tana area has similarly led to more frequent flooding and increased soil erosion. In both studies, wetland degradation has contributed to soil loss and agricultural land degradation, underscoring the crucial role of wetlands in flood regulation and soil conservation.

Another common impact is the significant decline in biodiversity. In the Muga Watershed, 93.7% of respondents observed a loss of biodiversity, which aligns with research by Lemma et al. (2024) in the

Baro-Akobo River Basin of western Ethiopia. Their study highlighted the loss of biodiversity due to wetland degradation, where the destruction of wetland ecosystems displaced many species of plants and animals. Both regions have witnessed the depletion of crucial habitats, disrupting local ecosystems and diminishing vital services such as water purification, nutrient cycling, and pollination, which are essential for supporting agriculture and food security.

The agricultural impacts of wetland loss are also strikingly similar to other areas. In the Muga Watershed, 91.3% of respondents reported a reduction in crop yields, a trend that reflects the role wetlands play in providing water regulation and nutrient cycling. This is similar with the findings from Hunegnaw et al. (2013) in the Ghibe River Basin in southern Ethiopia, where the degradation of wetlands resulted in diminished agricultural productivity. In the Ghibe River Basin, wetlands that once provided critical irrigation water and fertile soil have disappeared, leading to soil fertility loss and reduced agricultural yields, which threatens local food security. .

Water scarcity is another significant issue in both the Muga Watershed and other wetland areas of Ethiopia. In the Muga Watershed, 90% of respondents reported a decline in both the quantity and quality of water, particularly during dry seasons. This is comparable to the findings of Lautze et al. (2021) in the Omo-Turkana Basin, which is heavily impacted by wetland degradation. Their study found a notable decline in both surface and groundwater levels due to the loss of wetlands, exacerbating water scarcity for both agricultural and domestic use. The depletion of wetland resources in both regions highlights the essential role of wetlands in maintaining hydrological systems and securing a reliable water supply.

Resource conflicts are another shared consequence of wetland degradation in the Muga Watershed and Ethiopia's other wetland regions. In the Muga Watershed, 82.5% of respondents reported conflicts over access to dwindling resources. Similarly, Tadesse et al. (2024) observed similar tensions in the Awash River Basin of Ethiopia, where the degradation of wetlands led to increased competition for water and land resources. As wetlands in the Awash River Basin dried up, local communities began fighting over the remaining resources, much like the conflicts reported in the Muga Watershed. This intensifying competition for scarce resources further contributes to socio-economic instability in both regions.

The socio-economic effects of wetland degradation, particularly in the context of climate change, are also apparent in both regions. In the Muga Watershed, 88.7% of respondents linked wetland degradation to the impacts of climate change, which is aligned with the findings of Garedew et al. (2023) in the Bale Mountains region of Ethiopia. Their study revealed that wetland loss in the Bale Mountains has exacerbated climate change effects, including prolonged droughts and erratic rainfall patterns. In both regions, the loss of wetlands has undermined local communities' ability to adapt to and mitigate the impacts of climate change, further threatening their livelihoods and food security.

Despite these similarities, there are some contextual differences between the Muga Watershed and the Ethiopian study areas, particularly in terms of local governance and awareness regarding wetland management. In Ethiopia, Lemma et al. (2024) highlighted the growing recognition of wetland conservation efforts, particularly in the Gambella region, where community-based wetland restoration projects have been implemented successfully. In contrast, in the Muga Watershed, there may be a need for more concerted efforts to raise awareness and strengthen local governance structures to more effectively protect wetland resources.

4. Conclusions

The wetlands in the Muga Watershed have undergone significant degradation, driven by both anthropogenic and natural factors, resulting in adverse ecological and socio-economic impacts. The use of Remote Sensing (RS) and Geographic Information Systems (GIS) for Land Use/Land Cover (LULC) analysis over a 35-year period (1986–2021) revealed alarming trends of wetland loss, coupled with declines in forests and grasslands. Specifically, wetlands have been decreasing at a rate of 243.86 hectares annually, alongside reductions in forest cover (188.88 hectares per year) and grasslands (109.63 hectares per year). In contrast, agricultural land and built-up areas have expanded significantly, growing by 521.03 hectares and 21.34 hectares per year, respectively. Survey findings and key informant interviews identified population growth, farmland expansion, and overgrazing as the primary drivers of this degradation.

The consequences of wetland degradation in the Muga Watershed have been profound, including an occurrence of flood and erosion, loss of biodiversity, decrease of crop yield, shortage of quantity and quality water, conflicts over resource utilization, and occurrence of climate change. These findings underscore the urgent need for effective strategies to combat wetland degradation and promote sustainable management practices.

To address these challenges, a multi-faceted approach is required. Implementing comprehensive land use planning policies is crucial to prevent further conversion of wetlands for agriculture and urban development. Promoting alternative livelihoods, such as eco-tourism and sustainable fishing, can alleviate pressure on wetland resources while fostering economic growth. Strengthening legal and institutional frameworks for wetland protection will ensure the long-term preservation of these critical ecosystems. Moreover, efforts to restore degraded wetlands should include educating farmers and providing financial incentives to encourage sustainable agricultural practices. Improved livestock management strategies can help mitigate the impacts of overgrazing, while family planning initiatives can address population growth, reducing pressure on the watershed's natural resources.

Through these targeted measures, local and regional governments can mitigate wetland loss, promote environmental sustainability, and preserve the Muga Watershed’s ecosystems for future generations. These efforts are essential to ensuring both ecological health and the livelihoods of the communities that depend on these vital ecosystems.

Acknowledgement

We sincerely appreciate Debre Markos University for providing the essential facilities and resources that made this study possible. Our heartfelt thanks also go to the participating households for their invaluable cooperation and insights during the interviews. Additionally, we extend our deep gratitude to the Debaytilatgin District Agricultural Office for their unwavering support and collaboration throughout this research.

5. References

Agidie, A., Wondie, A., & Beneberu, G. (2024). The status of wetlands in seasonally flooded plains in eastern part of Lake Tana, Ethiopia. *International Journal of Bonorowo Wetlands*, *14*(2).

Alo, C. A., & Pontius Jr, R. G. (2008). Identifying systematic land-cover transitions using remote sensing and GIS: the fate of forests inside and outside protected areas of Southwestern Ghana. *Environment and Planning B: Planning and Design*, *35*(2), 280-295.

Assefa, W. W., Eneyew, B. G., & Wondie, A. (2021). The impacts of land-use and land-cover change on wetland ecosystem service values in peri-urban and urban area of Bahir Dar City, Upper Blue Nile Basin, Northwestern Ethiopia. *Ecological Processes*, *10*(1), 39.

Ballut-Dajud, G. A., Sandoval Herazo, L. C., Fernández-Lambert, G., Marín-Muñiz, J. L., López Méndez, M. C., & Betanzo-Torres, E. A. (2022). Factors affecting wetland loss: A review. *Land*, *11*(3), 434.

Barbier, E. B. (2011). Wetlands as natural assets. *Hydrological Sciences Journal*, *56*(8), 1360-1373.

Belay, T., & Mengistu, D. A. (2019). Land use and land cover dynamics and drivers in the Muga watershed, Upper Blue Nile basin, Ethiopia. *Remote Sensing Applications: Society and Environment*, *15*, 100249.

Biró, M., Czúcz, B., Horváth, F., Révész, A., Csatári, B., & Molnár, Z. (2013). Drivers of grassland loss in Hungary during the post-socialist transformation (1987–1999). *Landscape ecology*, *28*, 789-803.

Chamling, M., & Bera, B. (2020). Spatio-temporal patterns of land use/land cover change in the Bhutan–Bengal foothill region between 1987 and 2019: study towards geospatial applications and policy making. *Earth Systems and Environment*, *4*(1), 117-130.

Chanda, B., & Majumder, D. D. (2011). *Digital image processing and analysis*. PHI Learning Pvt. Ltd.

Cochran, W. G. (1977). Sampling techniques. *Johan Wiley & Sons Inc*.

Degife, A., Worku, H., Gizaw, S., & Legesse, A. (2019). Land use land cover dynamics, its drivers and environmental implications in Lake Hawassa Watershed of Ethiopia. *Remote Sensing Applications: Society and Environment*, *14*, 178-190.

Di Gregorio, A., & O'BRIEN, D. (2012). Overview of land-cover classifications and their interoperability. *Remote sensing of land use and land cover: Principles and applications*, 37-47.

Dixon, A., Wood, A., & Hailu, A. (2021). Wetlands in Ethiopia: lessons from 20 years of research, policy and practice. *Wetlands*, *41*(2), 20.

Dube, T., Dube, T., & Marambanyika, T. (2023). A review of wetland vulnerability assessment and monitoring in semi-arid environments of sub-Saharan Africa. *Physics and Chemistry of the Earth, Parts A/B/C*, *132*, 103473.

Garedew, K. F., Wedajo, M. A., & Belete, M. D. (2023). Spatio-temporal change of wetland and their effects on wetland biodiversity in Dinsho District, Bale Mountain Eco-Region, Southeast Ethiopia.

Gashaw, T., Tulu, T., Argaw, M., Worqlul, A. W., Tolessa, T., & Kindu, M. (2018). Estimating the impacts of land use/land cover changes on Ecosystem Service Values: The case of the Andassa watershed in the Upper Blue Nile basin of Ethiopia. *Ecosystem Services*, *31*, 219-228.

Gedefaw, A. A., Atzberger, C., Bauer, T., Agegnehu, S. K., & Mansberger, R. (2020). Analysis of land cover change detection in Gozamin District, Ethiopia: From remote sensing and DPSIR perspectives. *Sustainability*, *12*(11), 4534.

Geist, H., McConnell, W., Lambin, E. F., Moran, E., Alves, D., & Rudel, T. (2006). Causes and trajectories of land-use/cover change. In *Land-use and land-cover change: Local processes and global impacts* (pp. 41-70). Springer.

Gessesse, B., Bewket, W., & Bräuning, A. (2019). Land use and land cover transformation and its implication on land degradation: The case of Modjo watershed, Ethiopia. In *Extreme Hydrology and Climate Variability* (pp. 503-518). Elsevier.

Girma, R., Fürst, C., & Moges, A. (2022). Land use land cover change modeling by integrating artificial neural network with cellular Automata-Markov chain model in Gidabo river basin, main Ethiopian rift. *Environmental Challenges*, *6*, 100419.

Giweta, M., & Worku, Y. (2018). 'Reversing the Degradation of Ethiopian Wetlands': Is it Unachievable Phrase or A Call to Effective Action? *International Journal of Environmental Sciences & Natural Resources*, *14*(5), 136-146.

Gupta, R. P. (2017). *Remote sensing geology*. Springer.

Hailu, A., Mammo, S., & Kidane, M. (2020). Dynamics of land use, land cover change trend and its drivers in Jimma Geneti District, Western Ethiopia. *Land use policy*, *99*, 105011.

Harris, P. M., & Ventura, S. J. (1995). The integration of geographic data with remotely sensed imagery to improve classification in an urban area. *Photogrammetric engineering and remote sensing*, *61*(8), 993-998.

Hassen, E. E., & Assen, M. (2018). Land use/cover dynamics and its drivers in Gelda catchment, Lake Tana watershed, Ethiopia. *Environmental systems research*, *6*(1), 1-13.

Hunegnaw, G., Mengesha, H., Aimro, A., & Ferede, B. (2013). Wetlands ecosystems coverage, status and threats in the Abbay River Basin. *The Federal Democratic Republic of Ethiopia, Abay Basin Authority*, 50-58.

Hussien, K., Demissie, B., & Meaza, H. (2018). Spatiotemporal wetland changes and their threats in North Central Ethiopian Highlands. *Singapore Journal of Tropical Geography*, *39*(3), 332-350.

Kindu, M., Schneider, T., Teketay, D., & Knoke, T. (2013). Land use/land cover change analysis using object-based classification approach in Munessa-Shashemene landscape of the Ethiopian highlands. *Remote sensing*, *5*(5), 2411-2435.

Kingsford, R. T., Basset, A., & Jackson, L. (2016). Wetlands: conservation's poor cousins. *Aquatic Conservation: Marine and Freshwater Ecosystems*, *26*(5), 892-916.

Kumar, R., Kumar, A., & Saikia, P. (2022). Deforestation and forests degradation impacts on the environment. In *Environmental Degradation: Challenges and Strategies for Mitigation* (pp. 19-46). Springer.

Lautze, J., Gibson, J., & McCartney, M. (2021). *The Omo-Turkana Basin*. Routledge.

Lemma, B., Tesfaw, B., Desta, H., & Tessema, B. (2024). Studies on the conservation and sustainability challenges of the wetland resources of the Baro-Akobo River Basin in Gambella and Benishangul-Gumuz regions, Ethiopia. *Heliyon*, *10*(15).

Lillesand, T., Kiefer, R. W., & Chipman, J. (2015). *Remote sensing and image interpretation*. John Wiley & Sons.

Mathewos, M., Lencha, S. M., & Tsegaye, M. (2022). Land use and land cover change assessment and future predictions in the Matenchose Watershed, Rift Valley Basin, using CA-Markov simulation. *Land*, *11*(10), 1632.

Melese, S. M. (2016). Effect of land use land cover changes on the forest resources of Ethiopia. *International Journal of Natural Resource Ecology and Management*, *1*(2), 51.

Minale, A. S., & Belete, W. (2017). Land use distribution and change in lake Tana sub basin. *Social and Ecological System Dynamics: Characteristics, Trends, and Integration in the Lake Tana Basin, Ethiopia*, 357-373.

Murtessa, A. (2020). *Wetland change and its driving forces: the case of Halu district, Ilu Aba Bor zone,*

Ethiopia. Mettu University].

Nishri, A. (2011). Long-term impacts of draining a watershed wetland on a downstream lake, Lake Kinneret, Israel. *Air, Soil and Water Research*, *4*, ASWR. S6879.

Puyravaud, J.-P. (2003). Standardizing the calculation of the annual rate of deforestation. *Forest ecology and management*, *177*(1-3), 593-596.

Simane, B., Zaitchik, B. F., & Ozdogan, M. (2013). Agroecosystem analysis of the Choke Mountain watersheds, Ethiopia. *Sustainability*, *5*(2), 592-616.

Tadesse, B., Gelaw, F., & Shanko, D. (2024). Water Resources Use-Induced Conflicts in the Five Selected Basins of Ethiopia.

Tegaye, T. A. (2009). Natural lakes of Ethiopia.

Temesgen, H., Ketema, H., Kebede, G., Woldemariyam, F., & Tesfaye, G. (2025). The Golden Afromontane ecosystems at cross-road: Wetland-based upstream-downstream linkage in Genale Dawa River Basin. *Heliyon*, *11*(2).

Teshome, E., Randall, D., & Kinahan, A. (2011). The changing face of the Bale Mountains National Park over 32 years: a study of land cover change. *Walia*, *2011*(Special), 118-130.

Wubie, M. A., Assen, M., & Nicolau, M. D. (2016). Patterns, causes and consequences of land use/cover dynamics in the Gumara watershed of lake Tana basin, Northwestern Ethiopia. *Environmental systems research*, *5*, 1-12.

Xu, Y., Yu, L., Zhao, F. R., Cai, X., Zhao, J., Lu, H., & Gong, P. (2018). Tracking annual cropland changes from 1984 to 2016 using time-series Landsat images with a change-detection and post-classification approach: Experiments from three sites in Africa. *Remote Sensing of Environment*, *218*, 13-31.

Zekarias, T., Govindu, V., Kebede, Y., & Gelaw, A. (2021). Geospatial analysis of wetland dynamics on Lake Abaya-Chamo, the main rift valley of Ethiopia. *Heliyon*, *7*(9).

Zeleke, G., & Hurni, H. (2001). Implications of land use and land cover dynamics for mountain resource degradation in the Northwestern Ethiopian highlands. *Mountain research and development*, *21*(2), 184-191.

Zenebe, M. G., Fleskens, L., Ritsema, C., & Steenbergen, F. (2022). Basin-wide productivity and livelihood analysis of flood-based agricultural systems in African drylands: A case study in the Fogera floodplain. *Agricultural Water Management*, *261*, 107379.

Zewdie, W., & Csaplovies, E. (2015). Remote sensing based multi-temporal land cover classification and change detection in northwestern Ethiopia. *European Journal of Remote Sensing*, *48*(1), 121-139.